Arch. Metall. Mater. **69** (2024), 2, 525-534

DOI: https://doi.org/10.24425/amm.2024.149779

S.V. ALAGARSAMY[1], B. VINOTH[2*], D. DEEPAK[3]

EXPERIMENTAL INVESTIGATION ON WIRE ELECTRIC EROSION BEHAVIOUR OF SILICON DIOXIDE PARTICULATE REINFORCED COMPOSITE

The intend of current study was focused on the prediction of material removal rate (MRR) and surface roughness (SR) for the AA7050-SiO_2 composite during wire electric erosion or discharge machining (WEDM) process using a brass (Br) wire electrode. Here, stir casting process was employed to develop the AA7050 matrix composite with inclusion of 10wt.% SiO_2 particle reinforcement. The multi-objective optimization method of Technique for order preference by similarity to ideal solution (TOPSIS) approach has been applied to find out the optimal setting of input machining parameters such as peak current (I_p), pulse-on time (T_{on}) and pulse-off time (T_{off}). Furthermore, the significant effects of parameters were identified by analysis of variance (ANOVA). Taguchi L_9 (3^3) orthogonal design has been formulated to perform the experimental work. TOPSIS results stated that the optimal setting of I_p at 30 amps, T_{on} of 130 µs and T_{off} of 55 µs provide the better MRR with lesser SR. The ANOVA results noticed that I_p has the prime noteworthy parameter over the adopted responses having a contribution of 45.67%, followed by T_{on} (32.34%) and T_{off} (12.26%), respectively. The confirmation test was carried out by the optimal parameters setting to verify the predicted results. Finally, the scanning electron microscopy (SEM) test was carried out for the machined surface of the composite specimen and it was reveals that the formation of craters and recast layer thickness in the machined surfaces.

Keywords: AA7050; SiO_2; Stir casting; WEDM; Surface Roughness; TOPSIS; ANOVA

1. Introduction

Composite materials have evolved in prominence over the past several decades due to their adaptability in various sectors. Metal matrix composites (MMCs) are consistently in demand because of their unique features that set them apart from other types of materials [1]. MMCs are a feasible option for cast iron, which is often exploited in the manufacture of engines and brakes in the transportation sector, owing to their improved properties [2,3]. Aluminium, magnesium, and titanium are the metals that have been employed for MMCs in the majority of prior investigations. Aluminium matrix composites (AMCs) is the most prevalent form of MMCs. Due to their better performance in numerous industrial applications, aluminium and its alloys have been the subject of extensive investigation during the past decade. They are employed in the majority of automotive and aerospace applications because of their great strength and low weight and less cost, which result in lower fuel economy and good performance [4,5]. All of these characteristics increase the appeal of using aluminium and its alloys as the matrix phase for producing MMCs. In comparison to conventional materials, the AMCs with different reinforcements like SiC, TiO_2, ZrB_2, Al_2O_3, and B_4C has excelled in numerous sectors [6,7]. To make AMCs more affordable, a lot of research is being done to lower the price of reinforcing particles, which are expensive. AMCs are used more often for a variety of reasons, one of which is that they have lower cost requirements than other MMCs. As a result, AMCs potential for developing new applications is expanding. AMCs are often manufactured using a number of techniques, including powder metallurgy, stir casting, squeeze casting and spray deposition. Among these, stir casting is one of the most popular methods for making AMCs because of its ease of use, adaptability, cost-effectiveness, ability to produce large quantities, and ability to promote uniform distribution of reinforcing particles through stirring action [8]. The machining of AMCs seems to be very different from the machining of conventional metals in a number of ways. The material performance in the machining of AMCs is not only non-homogeneous and aniso-

[1] MAHATH AMMA INSTITUTE OF ENGINEERING AND TECHNOLOGY, DEPARTMENT OF MECHANICAL ENGINEERING, PUDUKKOTTAI-622 101, TAMIL NADU, INDIA
[2] MANGAYARKARASI COLLEGE OF ENGINEERING, DEPARTMENT OF MECHANICAL ENGINEERING, MADURAI-625 402, TAMIL NADU, INDIA
[3] PAAVAI ENGINEERING COLLEGE, DEPARTMENT OF AERONAUTICAL ENGINEERING, NAMAKKAL-637 018, TAMIL NADU, INDIA

* Corresponding author: sbvinothmech@gmail.com

tropic, but it also depends on matrix and reinforcement characteristics [9]. As the tool alternately interacts with the matrix and reinforcing elements, the reaction to machining these composites is completely different. Because the reinforcement particles constantly collide with the tool tip which leads to increase the tool wear and reduce the tool life during conventional machining of these composites [10,11]. Furthermore, by enhancing the surface finish of the product, traditional machining has failed miserably. The majority of production industries require intricate geometries, higher production rates, precise tolerances, and superior surface quality which are all accomplished by adopting non-traditional machining techniques. Accordingly, it is now possible to machine the new AMCs using the WEDM technique [12]. In WEDM, the metal is removed using a succession of high frequency pulse current of electrical discharges that are produced between the wire electrode and work piece through a incredibly tiny spark gap filled with a nonconductive dielectric fluid [13]. The cutting rate and surface quality are the most essential performances to assess the efficiency of WEDM. The WEDM efficiency mainly depends on a number of parameters like discharge current, voltage, pulse duration, pulse width, wire tension, wire feed and dielectric fluid, etc, [14, 15]. The key factors affecting WEDM efficiency include wire tension, dielectric fluid, discharge current, pulse width, and duration. Hence, this study investigated the effects of WEDM parameters on a newly developed AA7050 matrix composite. Recently, the many researchers [16-24] studied with Al based composites in WEDM to achieve a high MRR and low SR. Biing Hwa Yan et al. [16] have examined the machining performances like MRR and SR for the Al6063-Al_2O_3 composites during WEDM process. They results revealed that the better surface finish has achieved for 10 wt.% Al_2O_3 reinforced composite. Himanshu Prasad Raturi et al. [17] presented the effect of process parameters on MRR and SR for the Al6063-SiC-Al_2O_3 composites during WEDM process and the results indicated that the SR enhances and MRR declines with increase in wt.% of reinforcement due to improved the hardness. They also observed that increase in T_{on}, MRR increased and SR declined. Karthick et al. [18] employed TOPSIS approach to optimize the machining parameters on MRR and SR while WEDM of newer ($AlCoCrFeNiMo_{0.5}$) Al based composites filled with high entropy alloy (HEA) particles. They reported that the inclusions of HEA particles chiefly affect the adopted responses and also increase in reinforcement enhance the SR value. Reza Kashiry Fard et al. [19] studied the impact of several WEDM factors on cutting velocity and SR for the SiC filled Al matrix composites and they indicated that T_{on} and I_p have more significance factors against the responses. They also observed that lower T_{off} and higher T_{on} produced slight SR value due to increase in non cutting time leads to shallow craters. Selvakumar et al. [20] have optimized the WEDM parameters such as I_p, T_{on}, T_{off} and wire tension on cutting speed and SR for AA5083 using Taguchi method and the results depicted that the SR increased drastically with increase in T_{on} and I_p. Sakthi Sathasivam et al. [21] have explored the influence of WEDM factors over the MRR and SR for the Al6061– 6wt.% ZnO composites and they understood that the responses have mainly dominated by voltage and T_{on}, respectively. Dinesh Kumar et al. [22] investigated the machining characteristics of ZrB_2 (10 wt.%) reinforced AA7178 composites fabricated through stir casting method and they established that I_p (39.54%) and T_{on} (22.02%) had play a vital role for dominating the MRR and SR. Nelaturu Sai Preetham et al. [23] have fabricated the Al6061 matrix composites with addition of Al_2O_3 and Gr particles by stir casting route. They have studied the impact of WEDM parameters against the SR while machining of proposed composite and the results noticed that pulse duration has at most dominant factors than the others. Neel Kanth Grover et al. [24] investigated the SR of Al/(SiC+Gr+Fe_2O_3) composites during the WEDM process and observed that wire tension and peak current had more impact factors affecting the SR. They also reported that increase in I_p increase the SR due to greatest pulse energy produced more caters on the machined surface.

In the previous studies, we noticed that none of them had investigated the machinability studies on AA7050 matrix composite containing SiO_2 particles. Hence, the aim of the current attempt was to predict the machining behaviour of 10 wt.% SiO_2 reinforced AA7050 composite synthesized via stir casting route. The multi-objective method like TOPSIS approach has been adopted to find out the recommended parameter conditions for achieving superior MRR with lesser SR while WEDM process. Additionally, the significant consequences of machining parameters over the responses were determined by ANOVA statistical technique.

2. Experimental details

In this experiment, the matrix was taken as aluminium alloy 7xxx (AA7050), which was acquired from Coimbatore Metal Mart. Due to its high rigidity, superior strength to weight ratio, and natural ageing behavior, AA7050 is increasingly crucial for the manufacturing of shafts and gears, frames, wings, and fuselage components in the aerospace and automotive industries [25]. TABLE 1 depicted the chemical composition of aforementioned alloy. The reinforcement was utilized as silicon dioxide (SiO_2) particles with 30 μm particle size received from microtroniks lab chemicals. The composite specimen was fabricated by 10 wt.% of SiO_2 particles addition with matrix AA7050. Bottom pouring type stir casting method was adopted to synthesize the composite specimen.

TABLE 1

Composition of AA7050

Elements	Cu	Mg	Zn	Zr	Al
Wt.(%)	2.3	2.3	6.2	0.12	Remain

To achieve the homogeneous particle distribution stir casting technique was used to manufacture the composite in this investigation [26]. Initially, the weighted amount of AA7050 ingots was stored into graphite crucible and it was entirely

melted at 750°C using electrical furnace. A stainless steel stirrer is dipped into the molten alloy to start mechanical stirring at the mean time. This causes a vortex to form in the melt. To eliminate the moisture and increase the wettability with molten alloy, the weighted amount of SiO_2 (10 wt.%) particle was preheated for 1 hr at 300°C [27]. Then, the warmed SiO_2 particle was gradually added to the vortex of aluminium molten slurry. Constantly, the molten slurry was stirred for 15 min at 300 rpm [28]. Thereafter, composite slurry was poured into preheated mould and then permitted to cool at room temperature. The composite specimens were taken out of the mould after they had solidified, and a subsequent process was used to give them the desired shape. The process sequence of present work is depicted in Fig. 1.

In WEDM, the selection of inappropriate parameter can cause severe issues such as breakage cable, short circuits and work surface damage [29]. Therefore, the appropriate parameters selection plays an major role in the production schedule, and also MRR and SR are essential responses in WEDM. Several researchers have done the experimental work to improve the MRR and reduce the SR [30]. So that, the objective of this investigation is to achieve superior MRR with lower SR for the newly synthesized AA7050-SiO_2 composite. The experiments were carried out by varying the machining parameters listed in TABLE 2.

The synthesized AA7050-10wt.% SiO_2 composite was subjected to machining using WEDM setup (Make: Sprincut.

TABLE 2

WEDM parameters with its level

Notation	WEDM parameters	Units	Levels		
			1	2	3
I_p	Peak current	amps	30	60	90
T_{on}	Pulse-on time	µs	110	120	130
T_{off}	Pulse-off time	µs	45	55	65

win, Pune, India). A brass wire of 0.25 mm diameter was used as electrode material which is associated to negative polarity. An electrode made of Br wire that is generally alloyed with Cu (63-65%) and Zn (35-37%). According to earlier research, using Br instead of a Cu electrode increases the cutting rate and provide the better surface finish [31]. The dimensions of composite specimen were 100 mm long, 100 mm width and 10 mm thickness which is associated to positive polarity. The dielectric medium was taken as de-ionized water and it has maintained at 20°C. As per the parameter selection in TABLE 2, L9 orthogonal array (OA) has been designed by using Taguchi method. This OA design helps to reduce the number of experiments and it was provided in TABLE 3. The machining experiments were done as per L9 layout (TABLE 3) and each final cutting specimen size of 30 mm long, 10 mm width and 10 mm thickness, respectively. Mextech SRT-6200 surface roughness tester with 5 mm probe movement was used to assess the SR of the each machined

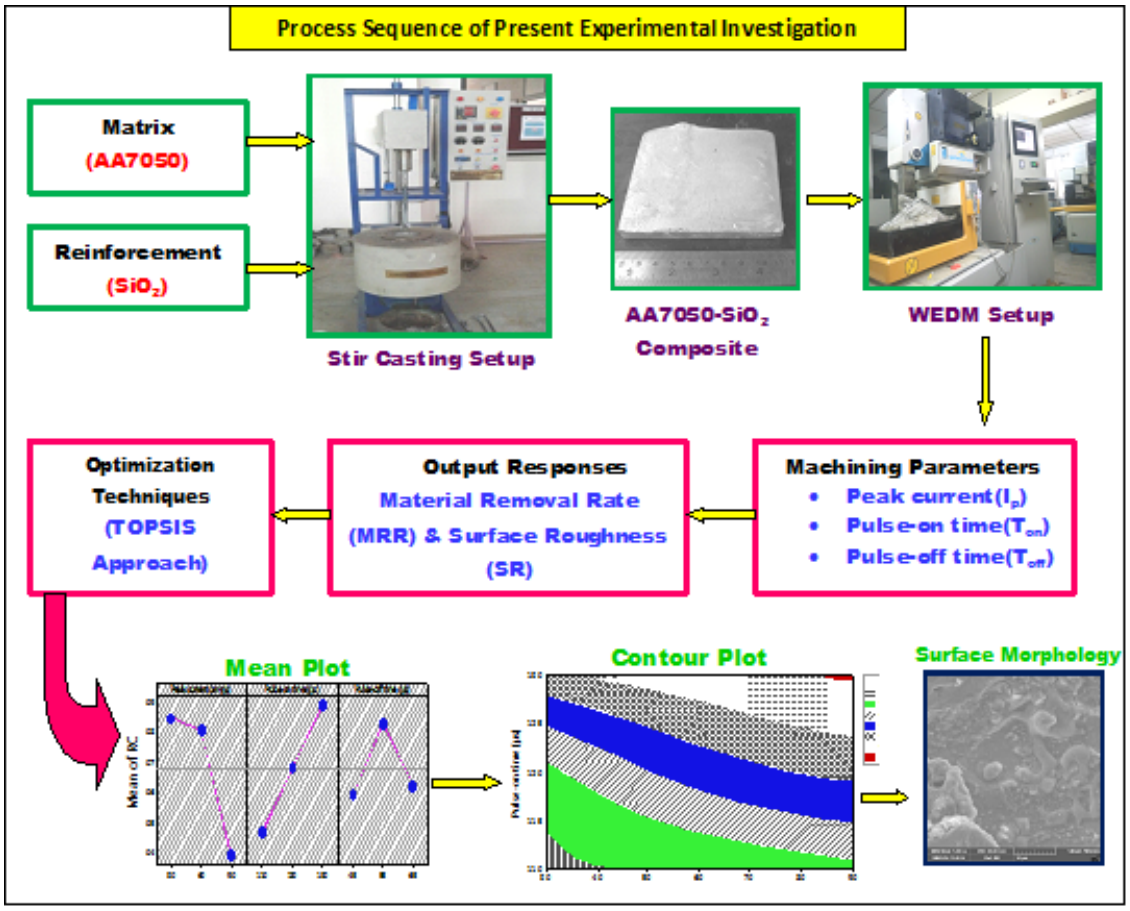

Fig. 1. Process sequence of present investigation

surface at different locations, and the average of these values were taken for further study. As usual, the MRR calculation was done by weight loss method. The work specimen was weighted before and after machining by using 0.001 g precision scale of electronic weighing machine. The given formula can be used to estimate the relative MRR,

$$MRR = \frac{W_i - W_f}{T_m}, \text{ g/min}$$

Where, W_i & W_f – initial and final weight of the work piece (g), T_m – machining time (min). TABLE 3 depicts the input parameters and their estimated responses.

TABLE 3

Input parameters and output responses

Ex. No	I_p (amps)	T_{on} (µs)	T_{off} (µs)	MRR (g/min)	SR (µm)
1	30	110	45	0.3270	3.251
2	30	120	55	0.3610	2.697
3	30	130	65	0.4830	2.564
4	60	110	55	0.3359	3.154
5	60	120	65	0.4251	2.815
6	60	130	45	0.5124	2.957
7	90	110	65	0.3589	4.361
8	90	120	45	0.4587	3.962
9	90	130	55	0.5342	2.846

3. Methodology – TOPSIS Approach

To solve multi-criteria decision making problems, TOPSIS is the finest traditional simple ranking method. Hwang and Yoon invented this technique in 1981 [32]. TOPSIS approach can be used to find out the appropriate option from the definite set of alternatives. Therefore, TOPSIS has been applied to determine the best machining parameter settings on superior MRR with lower SR for this investigation. In this approach, the appropriate alternative was pick up which should have nearer from the positive ideal solution and as well as far from the negative ideal solution [33]. To solve the multi-objective problems, the given steps to be involved in this approach are as follows,

Step 1: The first step is the m alternatives and n attributes are arranged in the form of decision matrix $D_{\max}$ as shown in below:

$$D = \begin{bmatrix} x_{11} & x_{12} & \cdots & \cdots & x_{1j} \\ x_{21} & x_2 & \cdots & \cdots & x_{2n} \\ \cdots & \cdots & \cdots & \cdots & \cdots \\ x_{i1} & x_{i2} & \cdots & x_{ij} & x_{in} \\ \cdots & \cdots & \cdots & \cdots & \cdots \\ x_{m1} & x_{m2} & \cdots & x_{mj} & x_{mn} \end{bmatrix}$$

where x_{ij} is the performance of value of i^{th} alternative in relation to the j^{th} attribute.

Step 2: Normalized matrix (r_{ij}) determined by normalizing the values within the decision matrix by using Eq. (1)

$$r_{ij} = \frac{x_{ij}}{\sqrt{\sum_{i=1}^{m} x_{ij}^2}} \tag{1}$$

where $i = 1,2,\ldots, m$ and $j = 1,2,\ldots, n$. x_{ij} – is the actual value of the i^{th} value of j^{th} experiment.

Step 3: Weighted normalized matrix is computed by multiplying the weights of each response with normalized matrix by using Eq. (2)

$$v_{ij} = r_{ij} \times w_j \tag{2}$$

where w_j – is the weight of the j^{th} attribute, $w_j = 0.5$, $i = 1,2,\ldots, m$ and $j = 1,2,.., n$. TABLE 4 provided the normalized and weighted normalized matrix.

TABLE 4

Normalized decision matrix

Ex. No	Normalized matrix		Normalized weight matrix	
	MRR	SR	MRR	SR
1	0.083220	1.091050	0.041610	0.545525
2	0.101425	0.750884	0.050713	0.375442
3	0.181562	0.678651	0.090781	0.339326
4	0.087811	1.026914	0.043906	0.513457
5	0.140641	0.818027	0.070321	0.409013
6	0.204338	0.902637	0.102169	0.451319
7	0.100248	1.963283	0.050124	0.981641
8	0.163753	1.620465	0.081876	0.810232
9	0.222095	0.836143	0.111047	0.418071

Step 4: Positive ideal solution (A^+) and negative ideal solution (A^-) are identified from the normalized weighted matrix by using Eq. (3) & (4)

$$A^+ = \left\{ \sum_{i=1}^{\max} v_{ij} \Big/ j \in J, \sum_{i=1}^{\min} v_{ij} \Big/ j \in J' \right\} \tag{3}$$

$$A^- = \left\{ \sum_{i=1}^{\min} v_{ij} \Big/ j \in J, \sum_{i=1}^{\max} v_{ij} \Big/ j \in J' \right\} \tag{4}$$

where, J is associated with the benefit parameters and J' – is associated with non-benefit parameters.

TABLE 5

Positive and negative ideal solution

Response	MRR	SR
V_j^+	0.111047	0.339326
V_j^-	0.041610	0.981641

Step 5: To determine the separation measure from positive and negative ideal solution are using Eq. (5) & (6)

$$S_i^+ = \sqrt{\sum_{j=1}^{n} \left(v_{ij} - A^+ \right)^2}, \; i = 1,2,\ldots,m \tag{5}$$

$$S_i^- = \sqrt{\sum_{j=1}^{n}\left(v_{ij} - A^-\right)^2},\ i = 1,2,...,m \qquad (6)$$

Step 6: The final step is to compute the relative closeness (C_i) from the separation measures by using Eq. (7)

$$C_i = \frac{S_i^-}{S_i^+ + S_i^-} \qquad (7)$$

The estimated separation measures, relative closeness and their rank are depicted in TABLE 6.

TABLE 6

Relative closeness and their rank

Ex. No	Separation measures		Relative closeness (C_i)	Rank
	MRR	SR		
1	0.217577	0.436116	0.667158	7
2	0.070318	0.606268	0.896070	2
3	0.020266	0.644195	0.969500	1
4	0.186627	0.46819	0.714994	6
5	0.080715	0.573347	0.876594	4
6	0.112344	0.533769	0.826123	5
7	0.645198	0.008514	0.013024	9
8	0.471809	0.176075	0.271769	8
9	0.078745	0.567831	0.878212	3

Step 7: Rank the RC (C_i) in ascending order and the maximum RC (C_i) value (TABLE 6) represented as rank 1 thus provide the appropriate parameters combination for arriving at better multi-objective results. The rank of RC (C_i) versus Ex. No are depicted in Fig. 2, and it ensure that the Ex. No 3 has obtained a larger RC (C_i) value (0.969500), which contains a appropriate conditions of machining parameter for providing superior MRR and lower SR.

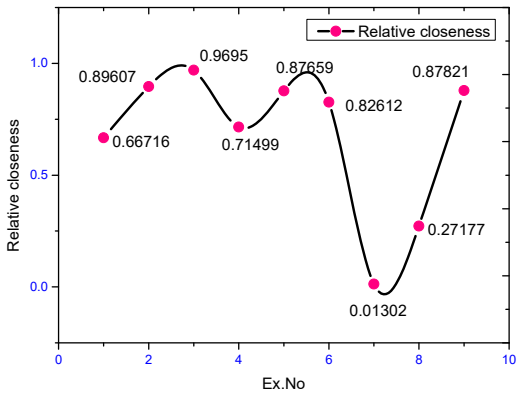

Fig. 2. Rank plot for RC

4. Results and discussion

4.1. Analysis of WEDM parameters on Responses

Figs. 3-5 depicted the response graphs for mean MRR, SR and RC against the machining parameters. From these graphs, we can understood that the influence of each process (WEDM) parameters over the responses. In Figs. 3-5, the parameter levels are illustrated in x-axis, while the mean values of response are depicted in y-axis. The response graph (Fig. 3) can be indicated that the greater MRR observed in high value of I_p (90 amps), high value of T_{on} (130 µs) and low value of T_{off} (45 µs). It can also be understood that with increase in current and pulse duration improve the MRR drastically due to high density spark generates more heat that utilizes to remove the metal from the work piece [34]. Figure 4 clearly found that low value of I_p (30 amps), high value of T_{on} (130 µs) and middle value of T_{off} (55 µs) produce lower SR. Additionally, it has been explored that increase in peak current delivers the high discharge energy thus produced enlarged craters on the machined surface resulted in increase the SR. The response graph for mean RC is illustrated in Fig. 5, and it clearly seen that the maximum RC value obtained at initial level of I_p (30 amps), high level of T_{on} (130 µs) and moderate level of T_{off} (45 µs). Hence, these levels of machining parameter are recommended for achieving superior MRR with slighter SR in proposed composite consisting of AA7050 with 10 wt.% SiO_2.

The response of mean RC value is depicted in TABLE 7. The sequence of noteworthy parameters has been identified from

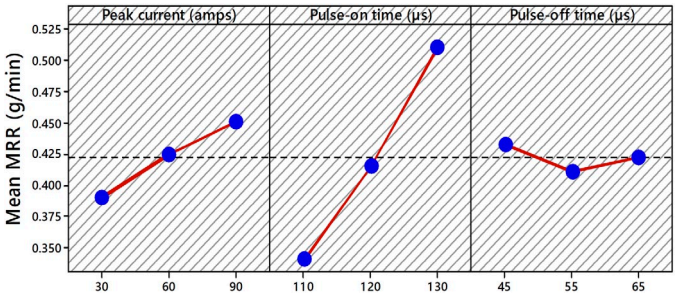

Fig. 3. Mean graph for MRR

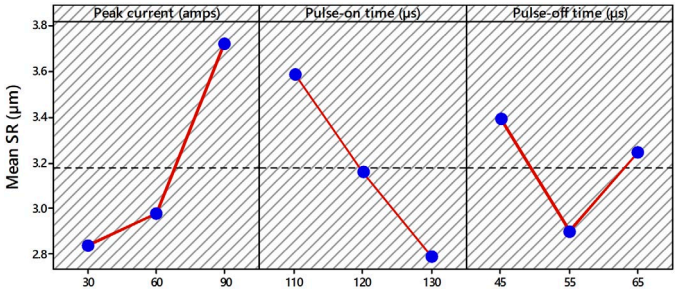

Fig. 4. Mean graph for SR

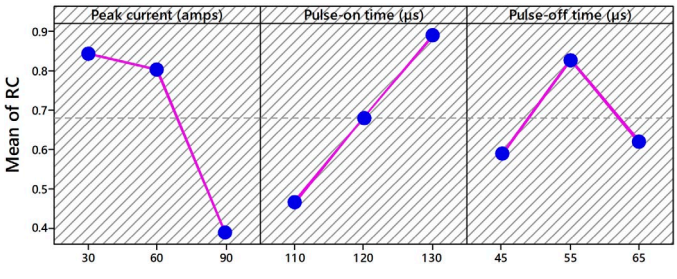

Fig. 5. Mean graph for RC

this table. In Table 7 clearly seen that the impact of parameters, such as I_p, T_{on} and T_{off} over the multiple responses (MRR and SR). Typically, the utmost significant parameters have greater delta value which is indicated as rank 1, followed by rank 2 and rank 3. Based on the delta value (TABLE 7), I_p has found to be the primary notable parameter with the delta value of 0.4566, subsequently by T_{on} ($\Delta = 0.4262$) and T_{off} ($\Delta = 0.2414$), respectively. The same findings have been already noticed by Alagarsamy et al. [33] and they concluded that I_p and T_{on} play a crucial role for improving the machining performances (high MRR with low SR) during the WEDM process.

TABLE 7

Mean table for RC

Level	I_p (amps)	T_{on} (µs)	T_{off} (µs)
1	0.8442	0.4651	0.5883
2	0.8059	0.6815	0.8298
3	0.3877	0.8913	0.6197
Delta (Δ)	0.4566	0.4262	0.2414
Rank	1	2	3
Average mean of RC = 0.679271			

4.2. Contour plot analysis

Fig. 6(a-c) illustrates the contour mapping of MRR with respect to machining parameters such as peak current (I_p), pulse-on time (T_{on}) and pulse-off time (T_{off}), respectively. From these plots, we had understood the interactive effect of WEDM parameters against the adopted responses. In Fig. 6(a) reveal the effect of I_p versus T_{on} with MRR. It clearly shows that the MRR linearly increasing with an increase in I_p and T_{on}. Here, the less MRR (0.33 g/min) found at initial level of I_p (30 amps) and T_{on} (110 µs). Furthermore, the MRR enhanced when I_p and T_{on} increased. So that, the higher MRR (0.53 g/min) has obtained at 90 amps of I_p with 130 µs of T_{on}. Generally, the greater I_p with longer pulse duration produce more spark energy that utilized to melt the work piece. Thus results in improving the MRR. Meanwhile, 125 µs of T_{on} produce 0.41 to 0.45 g/min of MRR at 30 amps of I_p. The interface effect of I_p with T_{off} on MRR is depicted in Fig. 6(b). It was seen that the maximum MRR (0.53 g/min) attained at 90 amps of I_p with 55 µs of T_{off}. Similarly, 90 amps of I_p with 45 µs of T_{off} produce higher MRR (0.49 to 0.53 g/min). It ensured that, the T_{off} has insignificant factor which means that the MRR doesn't depend on T_{off}. At middle level of I_p and T_{off} made MRR range from 0.33 to 0.37 g/min. At the same time, initial setting of I_p (30 amps) with high level of T_{off} (65 µs) gives the MRR from 0.45 to 0.49 g/min. In Fig. 6(c) depicts the influence of T_{on} and T_{off} with MRR. It was observed that the less MRR (0.33 g/min) found to be at 55 µs of T_{off} with T_{on} of 110 µs to 115 µs. Meanwhile, an increase in T_{on} from 110 µs to 130 µs, MRR significantly improved. At higher T_{on} (130 µs) with middle level of T_{off} (55 µs) gives maximum MRR (0.53 g/min). Similarly, the moderate MRR of 0.41-0.45 g/min observed at 125 µs of T_{on} with 65 µs of T_{off}.

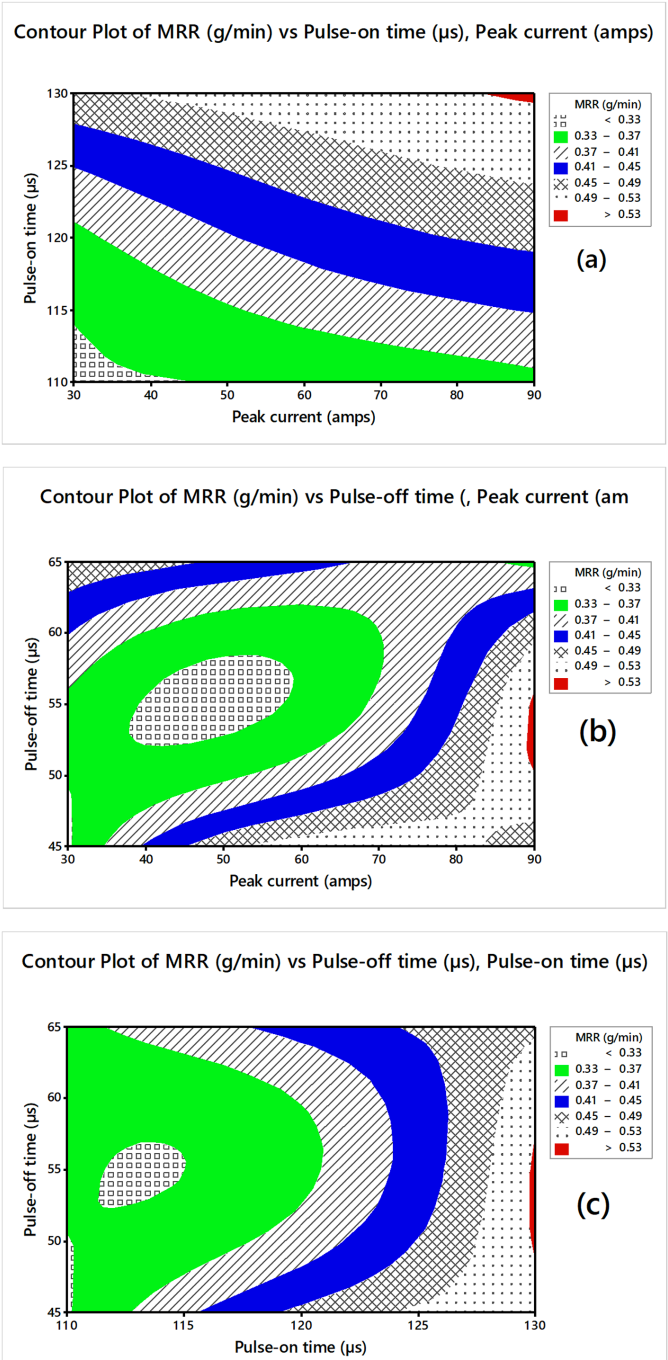

Fig. 6. Contour plot for MRR (a) I_p vs. T_{on}, (b) I_p vs. T_{off}, and (c) T_{on} vs. T_{off}

Fig. 7(a-c) displayed the contour graphs for SR of the machined composite with related to WEDM parameters, namely I_p, T_{on} and T_{off}. The influence of I_p and T_{on} on SR is shown in Fig. 7(a). It was obviously noticed that the SR increases when I_p increased and T_{on} decreased. So that, the higher SR (>4.2 µm) has produced at 90 amps of I_p and 30 µs of T_{on}. Initially, the lower SR (<2.7 µm) gives at 30 amps to 50 amps of I_p and 120 µs to 130 µs of T_{on}. Furthermore, an increase in I_p from 50 amps to 90 amps, the SR gradually improved. The moderate value of SR made at 80 amps of I_p and 120 µs of T_{on}. At the same time, the higher I_p with longer T_{on} has produced the minimum SR (2.7 µm-3.0 µm). In Fig. 7(b) demonstrates the effect of I_p and T_{off} on SR. It can

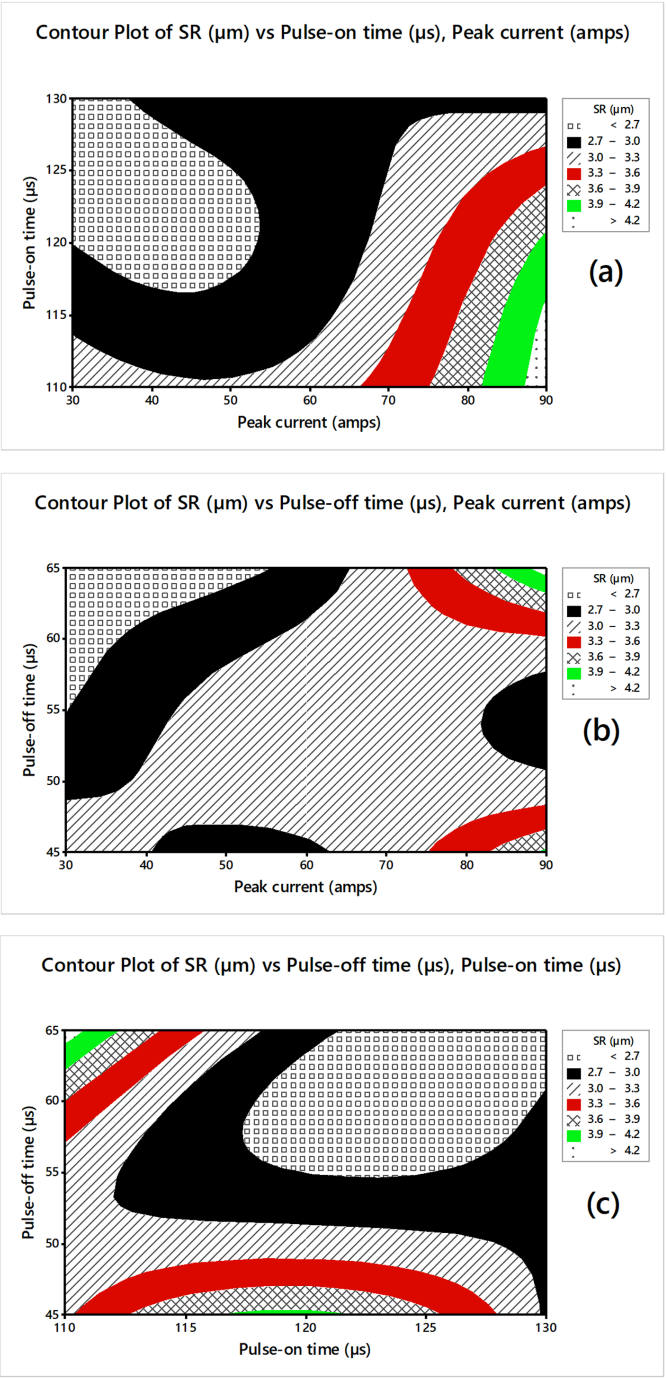

Fig. 7. Contour plot for SR (a) I_p vs. T_{on}, (b) I_p vs. T_{off}, and (c) T_{on} vs. T_{off}

be noticed that the lesser SR (<2.7 μm) gives at I_p of 30 amps and 65 μs of T_{off}. Similarly, the middle level of T_{off} (55 μs) and high level of I_p (90 amps) creates the SR in 2.7 μm -3.0 μm and also 50 amps of I_p and 45 μs of T_{off} developed the Same SR. The SR range of 3.0 μm-3.3 μm produces at all levels of I_p and T_{off}. Finally, the higher I_p (90 amps) and T_{off} (65 μs) gives the maximum SR (3.9-4.2 μm). At 80 amps of I_p and 45 μs of T_{off} produce the average SR of 3.3-3.6 μm, respectively. The interaction of T_{on} and T_{off} on SR is seen in Fig. 7(c). It has been exactly notice that the SR of the machined composite slightly reduced when an increase in T_{on} and T_{off}. Because of that, both factors are insignificant on SR during the WEDM process. But, the initial level of T_{on} (110 μs) and higher level of T_{off} (65 μs) gives the greater SR value of 3.9 μm-4.2 μm. At meantime, the lower SR (<2.7 μm) has attained from 120 μs to 130 μs of T_{on} and T_{off} from the level of 60 μs to 65 μs. The middle range of SR (3.3 μm-3.6 μm) formed at initial level of T_{on} and higher level of T_{off}.

4.3. Analysis of variance (ANOVA)

ANOVA is a statistical formula that is frequently used to assess the impact of independent variables on dependent outcomes. Determining the contribution percentage of each factor to the chosen responses is the major goal of this approach [35]. Since, in this investigation an ANOVA has been used to determine the significant effects of WEDM parameters like peak current (I_p), pulse-on time (T_{on}), and pulse-off time (T_{off}) on the MRR and SR for the newly developed AA7050-10 wt.% SiO_2 composite. The Minitab (version 17) software was used to obtain the ANOVA results for mean RC value and it was depicted in TABLE 8. The contribution percentage of each parameter against the adopted response is graphically displayed in Fig. 8. The sequential sum of squares (Seq. SS) value was used to calculate the percentage contribution of each parameter and the results (TABLE 8 and Fig. 8) make it clear that the peak current (I_p) is the most compelling factor for improving a superior MRR with better surface

TABLE 8

ANOVA for RC

WEDM parameter	DoF	Seq.SS	Adj.SS	Adj.MS	F-ratio	P (%)
I_p	2	0.38485	0.38485	0.19243	4.70	45.67
T_{on}	2	0.27252	0.27252	0.13626	3.33	32.34
T_{off}	2	0.10338	0.10338	0.05169	1.26	12.26
Error	2	0.08193	0.08193	0.04096	—	9.72
Total	8	0.84268	—	—	—	—
S = 0.202397 R-Sq = 90.28% R-Sq(adj) = 87.11%						

(DoF – Degrees of freedom, Seq.SS – Sequential sum of square, Adj. SS – Adjusted sum of square, Adj.SS – Adjusted mean square)

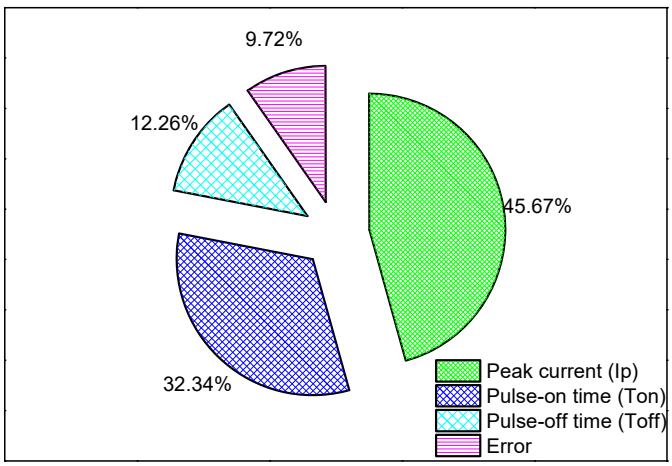

Fig. 8. Contribution of parameters on RC

finish. Therefore, the greater significant contributed parameter is I_p (45.67%), followed by T_{on} (32.34%) and T_{off} (12.26%), respectively. The similar result was previously found by Karthikeyan et al. [15]. The R square and adjusted R square are 90.28% and 87.11% respectively, and are very closer to the unity. Hence, the developed model exhibits higher capability prediction for the adopted responses.

4.4. Confirmation experiments

To confirm the improvement in the machining characteristics of newly proposed AA7050-10wt.% SiO_2 composite the confirmation experiment was performed by the optimal settings of WEDM parameters. The result of confirmation experiment was compared with the predicted results. The predicted result was estimated in Eq. (8).

$$\delta_{pre} = \delta_m + \sum_{k=1}^{n} (\delta_i - \delta_m) \tag{8}$$

where, δ_{pre} – predicted results, δ_m – the average RC value , δ_i – the RC value at the optimum conditions. The confirmatory results are depicted in TABLE 9, and it can be reveals that the experimental and predicted RC (C_i) values are 0.96950 and 1.20730, respectively. Based on the results (Table 9), the less error (0.19%) has been produced between the predicted and experimental results. Fig. 9 illustrates the probability graph for RC (C_i), and it can be seen that the results are placed within the limits, hence the developed model is able to predict with high accuracy.

TABLE 9

Confirmatory experiments

Parameter setting	Optimal level	MRR (g/min)	SR (µm)	RC (C_i)	Error
Experimental	$I_{p\text{-}1}T_{on\text{-}3}T_{off\text{-}3}$	0.4830	2.564	0.96950	0.19
Predicted	$I_{p\text{-}1}T_{on\text{-}3}T_{off\text{-}2}$	—	—	1.20730	

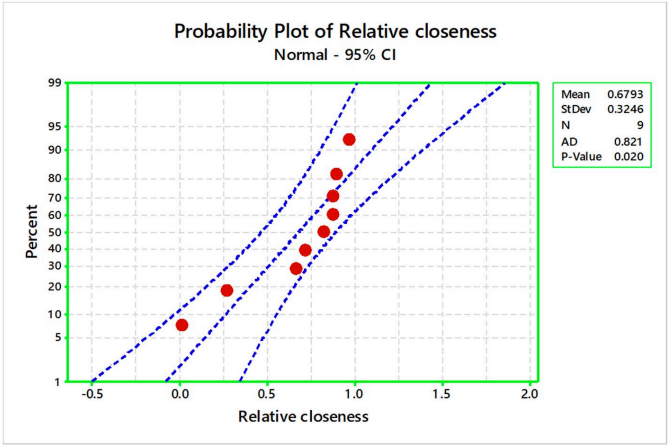

Fig. 9. Probability plot for RC

4.5. SEM morphology of Machined Surface

In order to examine the specifics of surface flaws like voids, craters, or splits, etc., the scanning electron microscopy ((VEGA3 TESCAN, Czech Republic) investigation was performed on the machined surfaces. Fig. 10(a) & 10(b) depicts the SEM images of the machined surface of AA7050-10wt.% SiO_2

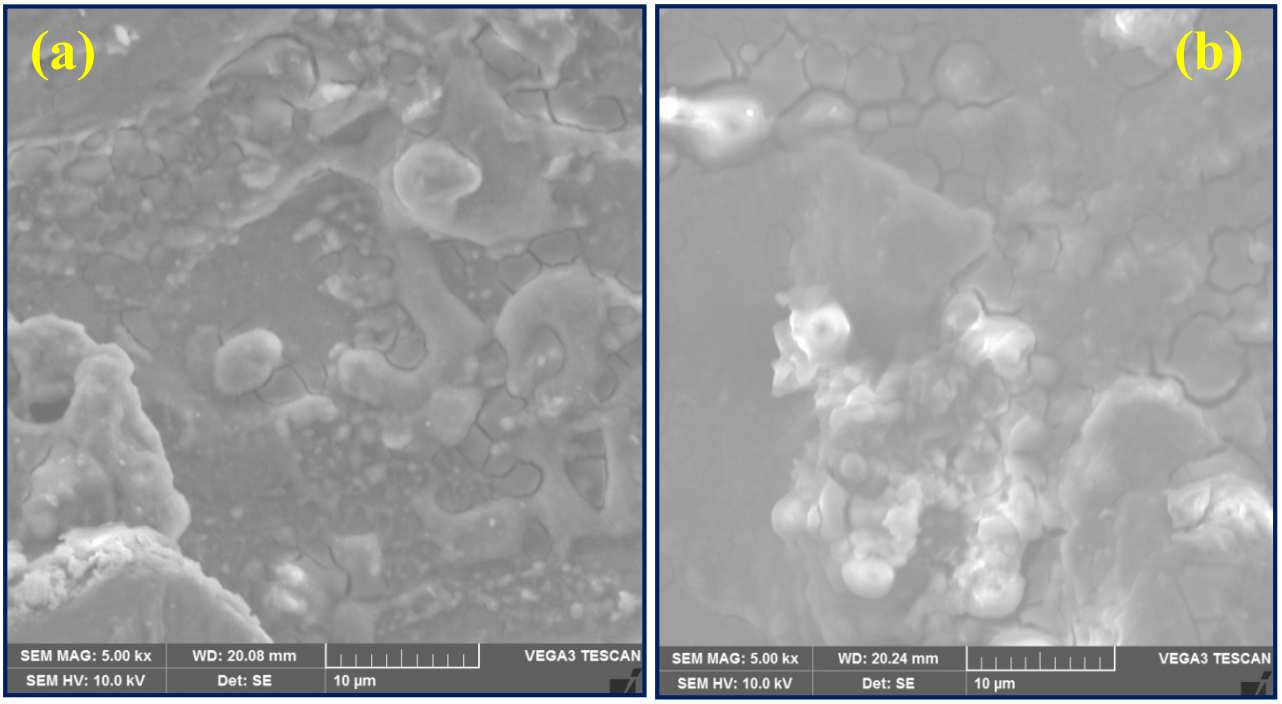

Fig. 10. SEM micrograph of the machined surface of AA7050/10wt.% SiO_2 composite (a) Initial parameter conditions, (b) Optimal parameter conditions

composite specimen. Fig. 10(a) displays the SEM image of the machined surface at initial settings of WEDM process parameter (I_p – 30 amps, T_{on} – 110 µs, and T_{off} – 45 µs). It clearly demonstrates that the machined surface has accumulated micropores and some fractures. The surface of the composite material had surface defects because of the greater pulse energy, which raised the temperature at the machined region. This causes more defects to appear on the machined surfaces. The SEM image of the machined surface in Fig. 10(a) also clearly evident the protrusion of the SiO_2 reinforcements. Moreover, rise in T_{on} causes the SR increases because to the increased density of the spark produced at higher I_p, which causes craters to develop on the surface [14]. The machined surface is also produced with the recast layer. The SEM image of the machined surface under the appropriate WEDM process parameter combinations (I_p – 30 amps, T_{on} – 130 µs, and T_{off} – 55 µs) is shown in Fig. 10(b). It is evident that higher spark density provided during the machining process in specific areas which causes the craters to form there. The surface becomes rougher with a longer T_{on} as a result of this deeper crater formation. On the other side, a longer T_{off} reduces the SR that may have come from the suitable flushing of melted materials that was achieved owing to an increase in flushing time. Appropriate flushing during extended T_{off} can certainly stop the re-deposition of material that was degraded during the spark [17]. Additionally, with moderate value of T_{off} creates fewer micropores on the machined surface. It was also realised that the recast layer only developed in a limited area because of the higher setting of T_{on}. As a result, the SR decreased as the recast layer decreased. Due to the existence of SiO_2 particles on the machined surface, this layer seemed to be uneven.

5. Conclusions

This investigation was performed to examine the WEDM characteristics of Al matrix composites by using TOPSIS approach. The given points can be derived from the experimental investigation:

1. Stir casting technique was effectively adopted to fabricate the defects free AA7050 matrix composite with incorporation of 10 wt.% SiO_2 particle as reinforcement.
2. The machinability study of fabricated composite was performed by WEDM process using Br wire electrode. As per Taguchi L_{16} orthogonal design, the machining was conducted.
3. TOPSIS approach has been utilized to yield the optimal setting of WEDM parameters such as peak current (I_p), pulse-on time (T_{on}) and pulse-off time (T_{off}) for obtain the higher MRR with lesser SR of the proposed composite.
4. The results from TOPSIS approach identified that the lower SR with greater MRR produced at 30 amps of I_p, 130 µs of T_{on} and 55 µs of T_{off}. The ANOVA results evident that I_p has play a vital role for dominating the responses with a contribution of 45.67%, followed by T_{on} (32.34%) and T_{off} (12.26%), respectively.
5. The interactive effects of parameters were illustrated in contour graphs and it has been observed that the superior MRR produced in higher values of I_p and T_{on}, while the slighter SR developed at lower value of T_{on} with higher value of I_p.
6. The surface texture of machined composite specimen was examined through scanning electron microscopy (SEM) and it was revealed that the recast layer thickness and craters are formed in the machined surfaces.
7. In the future, different WEDM parameters on composite machining performance may be optimised using other optimization techniques, such as machine learning algorithm and fuzzy logic approach.

REFERENCES

[1] Shoufa Liua, Yinwei Wang, T. Muthuramalingam, Anbuchezhiyan, Compos. Part B. Eng. **176**, 1-7 (2019).

[2] S.V. Alagarsamy, M. Ravichandran, Mater. Res. Express. **6**, 1-15 (2019).

[3] J. Lu, Z. Lu, J. Manuf. Sci. Eng. **132**, 1-7 (2010).

[4] Ashish K. Srivastavaa, Amit Rai Dixita and Sandeep Tiwari, Indian. J. Eng. Mater. Sci. **23**, 171-180 (2016).

[5] B.S. Yigezu, P.K. Jha, M.M. Mahapatra, Mater. Manuf. Process. **28**, 969-979 (2013).

[6] S.V.Alagarsamy, M. Ravichandran, Ind. Lubr. Tribol. **71**, 1064-1071 (2019).

[7] S. Suresha, B.K. Sridhara, Mater. Des. **34**, 576-583 (2012).

[8] P. Raveendran, S.V. Alagarsamy, M. Ravichandran, M. Meignanamoorthy, Surf. Rev. Lett. **28**, 1-11 (2021).

[9] D. Satishkumar, M. Kanthababu, V. Vajjiravelu, et al., Int. J. Adv. Manuf. Technol. **56**, 975-986 (2011).

[10] V.P. Goutham Murari, G.Selvakumar, C.Chandrasekhara Sastry, Metals. **10**, 1-31 (2020).

[11] S.V. Alagarsamy, M. Ravichandran, Mater. Test. **63**, 182-189 (2021).

[12] Aqueel Shah, Nadeem A. Mufti, Dinesh Rakwal, Eberhard Bamberg, J. Mater. Eng. Perform. **20**, 71-76 (2011).

[13] Thella Babu Rao, A.Gopala Krishna, Adv. Manuf. **1**, 265-275 (2013).

[14] J.W. Liu, T.M. Yue, Z.N. Guo. Mater. Manuf. Process. **24**, 446-453 (2009).

[15] A. Karthikeyan, S.V. Alagarsamy, C. Ilaiyaperumal, Surf. Rev. Lett. **29**, 1-11 (2021).

[16] Biing Hwa Yan, Hsien Chung Tsai, Fuang Yuan Huang, Long Chorng Lee, Int. J. Mach. Tool. Manuf. **45**, 251-259 (2005).

[17] S. Karthik, K. Soorya Prakash, P.M. Gopal, Sathiskumar Jothi, Mater. Manuf. Process. **34**, 759-768 (2019).

[18] Himanshu Prasad Raturi, Lalta Prasad, Mayank Pokhriyal, Vineet Tirth, J. Mech. Eng. **67**, 25-36 (2017).

[19] Reza Kashiry Fard, Reza Azar Afza, Reza Teimouri, J. Manuf. Process. **15**, 483-494 (2013).

[20] G. Selvakumar, G. Sornalatha, S. Sarkar, S. Mitra, Trans. Nonferr. Met. Soc. China **24**, 373-379 (2014).

[21] R.M. Sakthi Sadhasivam, K. Ramanathan, Sadhana. **46**, 1-10 (2021).

[22] S. Dinesh Kumar, M. Ravichandran, Silicon. **10**, 2653-2662 (2018).

[23] Nelaturu Sai Preetham, A. Muniappan, K.S. Jayakumar, T. Maridurai, Mater. Today: Proceed. (2021).
DOI: https://doi.org/10.1016/j.matpr.2021.07.328

[24] Neel Kanth Grover, Amresh Kumar, J. Indian Chem. Soc. **97**, 339-344 (2020).

[25] P. Vignesh, S.V. Alagarsamy, P. Raveendran, H. Saravanan, K. Karthikeyan, Mater. Today: Proceed. **47**, 4121-4125 (2021).

[26] G. Veerappan, M. Ravichandran, S.V. Alagarsamy, V. Mohanavel, Surf. Topogr.: Metrol. Prop. **10**, 1-12 (2022).

[27] K. Velavan, T. Muthukrishnan, T.Srinivasan, P. Sethuvelappan, N. Ramanan, J. Phys.: Conf. Ser. 2070, 1-9 (2021).

[28] J. Chandrasheker, N.V.S. Raju, AIP. Conf. Proc. **2648**, 1-8 (2022).

[29] Anand Babu Kumba, P. Venkata Ramaiah, U.P.B. Sci. Bull., Series D. **81**, 169-186 (2019).

[30] S. Saravanan, P. Senthilkumar, M. Ravichandran, N. Shivasankaran, Mater. Res. Express. **5**, 1-10 (2018).

[31] Maher, A.A.D. Sarhan, M.H. Abd Shukor. Int. J. Adv. Manuf. Technol. **76**, 329-351 (2015).

[32] Yue-Peng Zeng, Chiang-Lung Lin, Hong-Mei Dai, Yan-Cherng Lin, Jung-Chou Hung, Process. **9**, 1-18 (2021).

[33] S.V. Alagarsamy, P. Raveendran, M. Ravichandran, Silicon. **13**, 2529-2543 (2020).

[34] K. Subramaniam, A. Natarajan, N. Vinayagam, S.J. Muthiya, et al., SAE Tech. Pap. 2020-28-0426 (2020).

[35] S.V. Alagarsamy, M. Ravichandran, S. Dinesh Kumar, et al., Mater. Today: Proceed. **27**, 853-858 (2020).

[36] S.V. Alagarsamy, M. Ravichandran, Mater. Res. Express. **7**, 1-17 (2020).